HHS Public Access

Author manuscript

Fuel (Lond). Author manuscript; available in PMC 2018 April 15.

Published in final edited form as:

Fuel (Lond). 2018 April 15; 218: 306–315.

Some relevant parameters for assessing fire hazards of combustible mine materials using laboratory scale experiments

Charles D. Litton, **Inoka E. Perera***, **Samuel P. Harteis**, **Kara A. Teacoach**, **Maria I. DeRosa**, **Richard A. Thomas**, and **Alex C. Smith**

National Institute for Occupational Safety and Health, Pittsburgh Mining Research Division, 626 Cochrans Mill Road, PO Box 18070, Pittsburgh, PA 15236, USA

Abstract

When combustible materials ignite and burn, the potential for fire growth and flame spread represents an obvious hazard, but during these processes of ignition and flaming, other life hazards present themselves and should be included to ensure an effective overall analysis of the relevant fire hazards. In particular, the gases and smoke produced both during the smoldering stages of fires leading to ignition and during the advanced flaming stages of a developing fire serve to contaminate the surrounding atmosphere, potentially producing elevated levels of toxicity and high levels of smoke obscuration that render the environment untenable. In underground mines, these hazards may be exacerbated by the existing forced ventilation that can carry the gases and smoke to locations far-removed from the fire location. Clearly, materials that require high temperatures (above 1400 K) and that exhibit low mass loss during thermal decomposition, or that require high heat fluxes or heat transfer rates to ignite represent less of a hazard than materials that decompose at low temperatures or ignite at low levels of heat flux. In order to define and quantify some possible parameters that can be used to assess these hazards, small-scale laboratory experiments were conducted in a number of configurations to measure: 1) the toxic gases and smoke produced both during non-flaming and flaming combustion; 2) mass loss rates as a function of temperature to determine ease of thermal decomposition; and 3) mass loss rates and times to ignition as a function of incident heat flux. This paper describes the experiments that were conducted, their results, and the development of a set of parameters that could possibly be used to assess the overall fire hazard of combustible materials using small scale laboratory experiments.

Keywords

Fire hazards; Combustible; Mine materials

1. Introduction

Fires represent one of the most significant hazards that can occur in underground mines, with significant potential for injury and loss of life. Materials that smolder and burn can expel large quantities of toxic gases and smoke into the mine's ventilation airflow where these products are transported to distances often far-removed from the seat of the fire. When

*Corresponding author. eperera@cdc.gov (I.E. Perera).

smoldering fires are left unattended, their eventual transition to flaming and subsequent fire growth and flame spread render the underground atmosphere untenable and cause disastrous consequences for both life and property. Mining involves the use of many types of combustible materials that are brought underground to facilitate the mining process. Such materials include brattice curtains, conveyor belts, mine foams and sealants, electrical insulating materials, and so on, with many different chemical formulations possible for each. However, along with providing their necessary functions to the mining activities, many, if not most, of these combustible materials may represent significant fire hazards if not selected with criteria that are intended to minimize any potential dangers.

Some of these materials are required by regulations to pass stringent tests for flame spread, such as conveyor belts, while others may have to be certified as fire-resistant based upon the results of other standard laboratory tests [1]. While fire resistance and flame spread are important parameters to limit the potential hazards that fires involving these materials may present, there exist other properties relevant to the material and also to the resultant effects of their combustion that are quite important. For instance, the relative ease or difficulty of materials to thermally decompose or their response to various levels of heat flux and/or elevated temperatures that result in their ignition are important parameters. As materials thermally decompose during their smoldering stages, smoke and potentially toxic gases may be produced that can render the mine air untenable and result in severe adverse health effects. Subsequent to ignition, flaming materials tend to generate smoke with higher carbon content (i.e., black carbon) and additional toxic gases, and as the fire intensity increases, the production of smoke and toxic gases also increases.

Prior research efforts have generated data on the thermal decomposition and ignition properties of a wide range of combustible materials, and much of this research has also addressed the generation of smoke and toxic gases, primarily subsequent to ignition and as a function of the fuel-to-air ratio [2–5]. Litton et al. studied the ignition and flame spread properties of a variety of noise abatement materials in both medium- and large-scale experiments and developed the concept of a heat parameter to assess the relative risk of flame spread [6]. Pa-ciorek et al. [7] catalogued the yields of over 500 toxic gas compounds during the thermal decomposition of numerous combustible mine materials [8,9]. This previous research spans the period from the mid-1970s to the mid-1990s, and while much of this work remains relevant, very little research has been conducted more recently to measure and quantify the hazards from the many new combustibles used in today’s underground mines. In addition, the testing and evaluation of some materials, in particular, conveyor belts, has most recently been accomplished only through large-scale testing that is difficult and expensive, while smaller, laboratory-scale studies have been sorely lacking.

The research described in this report seeks to fill that void through the development of a suite of smaller-scale laboratory experiments that quantify the various hazards mentioned above via parameters that are relevant to a diverse range of combustible mine materials. Such parameters will include a smoke hazard parameter (SHP) that defines both the relative smoke obscuration level and the particle surface area that can be related to adverse health effects; toxicity indices (TI) that define weighted sums of the toxic gases produced both during flaming and non-flaming combustion; and thermal parameters (TP1 and TP4, which

explained in Theory section) that define a combustible material's ease of ignition and subsequent fire intensity. All of these parameters can be used to rank the materials in terms of the hazards they present, from low hazard to high hazard. The paper concludes with a discussion of the potential utility of these parameters for an overall hazard evaluation that may be used to assess potential risk, and describes how this evaluation may lead to the selection of those materials that pose the lowest overall risk.

2. Experimental

In order to address the various hazards that fires and developing fires may present, it was necessary to conduct experiments using two distinct experimental arrangements:

1. A radiant panel to quantify the material's ease of ignition and heat of gasification as a function of known heat flux at the material surface; and
2. A smoke chamber for quantifying the yields of toxic gases and smoke, along with the relevant smoke properties, for both flaming and non-flaming combustion.

The experimental configurations and methodologies used for the radiant panel experiments and the smoke chamber experiments, along with detailed results, are presented by Harteis et al. and Litton et al., respectively [6,9]. These experiments and the parameters derived from the radiant panel and smoke chamber experiments will be discussed and summarized in the following sections and then used to assess the overall fire hazard.

2.1. Radiant panel experiments and theory

2.1.1. Experiments—A radiant panel apparatus was constructed to determine the various combustion properties of the mine materials during the thermal decomposition and ignition stages of combustion. A metal structure was fabricated to serve as the base frame for the test apparatus. Two layers of ¼-in-thick, high temperature millboard were installed to provide a barrier between the radiant heater and the test frame, and to protect the surroundings from heat generated by the radiant panel. The radiant panel selected for this application, a Raymax 2030 (Watlow),[M] was mounted vertically, directly in front of the millboard, attached to the base frame. A 240-volt, single-phase, variable output transformer provided electrical power to the radiant panel. Eight type-K thermocouples were installed in the fume stack above the apparatus to measure the gas temperatures. A gas sampling tube connected to carbon monoxide (CO) and carbon dioxide (CO_2) analyzers measured the amount of CO and CO_2 generated during testing. The radiant panel apparatus is shown in Fig. 1.

Prior to the material testing, the radiant panel was calibrated using a Hukseflux USA1 heat flux gauge. The gauge was mounted horizontally, 2 in from the center of the radiant panel, to measure the heat flux as a function of applied voltages to the radiant panel. Sixteen materials were selected for testing: 4 brattice materials, 2 sealants, 7 conveyor beltings, and 3 woods. For the wood and conveyor belt materials, a ¼-in-diameter by 2½-in-deep pilot hole was

[M]ention of specific brands or manufacturers does not imply endorsement by The National Institute for Occupational Safety and Health.

drilled into the material to accommodate the metal stand used to hold the material in place during the test. For the brattice, a material holder was designed with metal clips to hold the material in place. For the foam sealant material, a holder was designed with a thin rod to hold the material. Fig. 2 shows one of the metal stands with the sample material in place.

Each material was weighed and fastened to the holder. The test holder and material were placed on a load cell, 2 in from the radiant panel. The load cell was used to determine the weight loss of the material over time for each test. A pilot flame was located just above the material to ignite the flammable gases emitted from the material. Power to the radiant panel was turned on to begin the test. If the material ignited before 5 min had elapsed, the time would be recorded and noted as ignition time. If the specimen failed to ignite after 5 min had elapsed, the test was considered complete and recorded as a non-ignition. If the pilot flame extinguished during the test, a note was made of this and the test repeated. The test was repeated with a new sample of the material at heat fluxes above and below the initial test heat flux to determine the minimum heat flux required for ignition, time to ignition, and mass loss rates at the various heat fluxes. These parameters were then used to calculate the heats of gasification and three thermal parameters that were used to rank the materials from the low thermal hazard to high thermal hazard. Low hazard materials are relatively difficult to ignite, and if ignited, do not burn vigorously; while high hazard materials ignite easily, and once ignited burn vigorously.

2.1.2. Theory—For a solid surface, assumed to be of semi-infinite thickness, the surface temperature, T_s, as a function of time, t, when exposed to a constant external radiant heat flux, q_e'', is given by the expression [Carslaw, 1959]

$$T_s = T_0 + q_e'' \cdot \left[\frac{4t}{\pi K \rho C_p} \right]^{1/2} \quad (1)$$

where:

T_0 is the initial surface temperature (K),

κ is the solid thermal conductivity, kw/(m K),

ρ is the density of the solid, g/m^3,

c_p is the heat capacity of the solid, kJ/(g K), and q_e'' is in kW/m^2.

As the surface temperature and the temperature of the solid mass beneath the surface begin to increase, the solid begins to thermally decompose resulting in the expulsion of fuel vapors at the surface. If the heat flux is sufficiently high, then at some point sufficient fuel is generated to form a flammable mixture at the surface and this mixture subsequently ignites. If the surface temperature at the instant of ignition is defined to be T_{ig}, then a lumped parameter containing the material thermal properties can be defined as a Thermal Response Parameter (TRP) given by [2a];

$$TRP=(T_{ig}-T_0)\cdot(K\rho C_p)^{1/2} \quad (2a)$$

Substituting this expression into Eq. (1) and rearranging yields the alternate expression in terms of measurable quantities

$$TRP=(4/\pi)^{1/2}\cdot q_e''\cdot(t_{ig})^{1/2} \quad (2b)$$

where t_{ig} is the time (seconds) at which the combustible fuel vapors ignite above the surface of the solid. For *TRP*, the smaller its value, the easier it is for the material to ignite and subsequently burn and, as a result, the hazard associated with the ignition process should vary in some inverse manner with *TRP*.

Once ignition occurs, the surface of the combustible burns generating heat and, if extensive enough, flame spread across the surface results, producing an ever-increasing heat release rate, Q_f (kW). The resulting levels of Q_f are proportional to the mass generation rate of fuel vapors and the heat of combustion of the solid, or

$$Q_f=m_f''\cdot A_s\cdot H_c \quad (3)$$

where:

m_f'' is the mass flux of fuel vapors from the solid surface (g/(m^2 s))

A_s is the sample surface area (m^2) and

H_c is the heat of combustion of the solid combustible (kJ/g).

The magnitude of the heat release rate depends upon the rate at which the solid decomposes, producing fuel at the surface, and this rate of fuel production depends, in turn, on the rate at which the solid is being heated. During active burning, the rate at which the surface is heated is due primarily to the radiative heat to the surface that is continuously supplied by the flame. In order to assess the levels of mass flux that can be generated from one material to the next and, hence, the levels of heat that can be produced from a flaming fire, the use of another combustible property, the heat of gasification, h_g, in kJ/g can be used. The heat of gasification is defined as the ratio of incident heat flux divided by the mass flux of fuel vapors, or

$$h_g=q_e''/m_f'' \quad (4)$$

By measuring the mass loss rate of the solid combustibles at different levels of incident heat flux, the heats of gasification for each can then be determined, and for the heat fluxes

actually encountered during flaming combustion, the mass flux will vary inversely with h_g. Consequently, for different materials the relative heat release rates that would result from burning of a constant combustible surface area are proportional to ratio of heat release rate to heat of gasification, or

$$Q_f \alpha H_c/h_g \quad (5)$$

During an active flaming fire, the hazard will increase as the heat release rate increases, and for different combustible materials, the hazard will vary with the size of fire that can be generated from that material. Consequently, the hazard will increase as the ratio, H_c/h_g, increases.

If the ignition hazard and the flaming hazard are combined into one hazard parameter, then this parameter would vary directly with Eq. (5) and inversely with *TRP* as defined in Eqs. (2b) and (3) above. At the minimum, two possibilities exist—i.e., that the combined hazard varies in 1) a multiplicative manner or in 2) an additive manner. For the multiplicative case, the Thermal Parameter *TP1* is given by the expression

$$TP1=10^4 H_c/(h_g \cdot TRP) \quad (6)$$

For the additive alternative, the Thermal Parameter *TP4* is given by the expression

$$TP4=10H_c/h_g+100H_c/TRP \quad (7)$$

Both of these parameters scale in the same manner and can be used to assess the potential ignition and fire intensity hazards from the combustible materials. More details of this research can be found in the paper by Harteis et al. [9]. These parameters are listed in Table 1 for the materials tested in this portion of the research. There are no values for *TP1* in the following Tables for sample numbers 3 and 9 because no values were obtained for their heats of gasification, h_g. The lack of these values also affects the values shown for *TP4,* however they are included in Table 1, because the effect of heat of gasification on the TP4 number on sample 3 and 9 would be negligible.

The average thermal parameter values shown in Table 1 vary over a fairly large dynamic range, and it is not clear just from the tabular values if either *TP1* or *TP4* is a better measure than the other, or if there is any appreciable difference for the combined hazards of ignition and fire intensity. To assess how each of these parameters scale with the other, *TP4* is plotted vs *TP1* in Fig. 3.

From Fig. 3, it is apparent that both parameters correlate and that, in defining a combined parameter that represents an estimate of the combined hazard, it makes little difference

which one is chosen. This result can also be demonstrated by ranking the various materials from low hazard to high hazard based upon the values of either *TP1* or *TP4*. In order to show this comparison, the samples are designated with numbers 1 through 16 and then ranked from low hazard to high hazard based upon their respective values of *TP1* and *TP4*. The results of this ranking are shown in Table 2.

Based upon this comparison, one of the line brattices tested, #4, represents the lowest hazard while one of the sealants, #6, represents the highest hazard. It is worth noting that the wood samples ranked on the high end of the hazard comparison and that oak was ranked somewhat less hazardous than either of the pine woods tested.

2.2. Smoke chamber experiments and theory

2.2.1. Experiments—Experiments were conducted using a standard Underwriters Laboratory Inc. (UL 268) smoke chamber connected to a combustion chamber in which the samples were either burned or thermally decomposed. The experimental procedure is described in detail elsewhere and for these studies mass loss of the samples was also continuously measured using calibrated Daytronic load cells [10]. Samples were typically in the shape of small rectangular solids with initial masses ranging from a low of 0.70 g (Silent Seal Foam) to a maximum of 33.7 g (conveyor belt 8020–0168 M) with an average of 11.8 g for all experiments. Once inside the smoke chamber, the gases and aerosol were mixed uniformly using two small circulating fans. Within the smoke chamber, optical density of the aerosol was measured over a 1.48-m optical path length using an incandescent lamp and a standard photocell with a spectral response matching the spectral response of the human eye. Two multi-gas Ibrid MX-6 sensors were placed inside the smoke chamber that allowed for continuous measurement of the toxic gases CO, HCl, HCN, H_2S, NH_3, SO_2, NO and NO_2, and VOCs through an internal microprocessor. During the experiments, the combustion aerosols were continuously extracted from various ports on the smoke chamber using metal tubes inserted into the top of the smoke box and flowed to various measuring devices.

These devices included discrete angular scattering at a wavelength of 532 nm using a precisely machined scattering chamber described in detail in separate manuscripts [11–13]. The normalized angular scattering data were subsequently used to derive the radius of gyration, R_g, and fractal dimension, D_f, of the fractal aggregates produced. One port was connected to either a TSI DustTrak 8520 or 8530 for continuous mass measurement using calibration factors defined previously. Another port was connected through a 0.68-m light extinction tube where light extinction at a wavelength of 532 nm was continuously measured. The aerosols were then flowed through an EcoTech nephelometer where the total scattering was measured at a wavelength of 520 nm.

Samples were also flowed to a prototype OPTION sensor that consisted of a well-defined ionization chamber and an optical scattering chamber for discrete measurements of angular scattering at 15° and 30° at a wavelength of 635 nm. The ionization chamber and angular sensitivities were obtained in units of voltage change per unit mass concentration [15]. The ratio of ionization response to optical scattering response and the ionization chamber response were used to determine the average number concentration of aggregate particles,

average mass of an aggregate, primary particle diameter, and number of primary particles per aggregate as detailed in previous reports.

3. Gas analysis and development of a toxicity index

Previous studies analyzed combustion product gases and developed an expression to estimate the toxicity of combustion product gases using the Immediately Dangerous to Life and Health (IDLH) concentration for each toxic gas as a weighting factor [DeRosa 1989]. Their development of this Total Relative Toxic Hazard (TRTH) and a simpler toxicity index (TI) is as follows:

Let X denote a particular toxic gas produced during the combustion of a particular material Z. For each toxic gas, there exists a parameter, Y_X, called the yield, and expressed in units of grams of gas produced per gram of material consumed during the combustion process (g/g). Assuming that the gas mixes completely with the air into which it is expelled during the combustion of the sample, then the resultant concentration is given by

$$X\left(\frac{g}{m^3}\right) = Y_x \cdot \left(\frac{dM_z}{dt}\right) \cdot \left(\frac{t}{V}\right) \quad (8)$$

Where

dM_Z/dt is the rate of mass loss of the sample material Z (g/s);

t is the time for combustion of the sample material (s); and

V is the volume into which the gas is expelled (m^3).

The concentration of X can be converted to parts per million ppm by dividing X in Eq. (8) by a constant, C_X, that is equal to the molecular weight of the gas, M_X, in grams, divided by 22,414, or

$$X(ppm) = \left(\frac{Y_x}{C_x}\right) \cdot \left(\frac{dM_z}{dt}\right) \cdot \left(\frac{t}{V}\right) \quad (9)$$

Eq. (9) is strictly applicable only to an enclosed system at constant pressure. For many systems, and for mines in particular, the gas mixes with a flowing airstream. When this is the case, the concentration of toxic gas, X, is given by

$$X(ppm) = \left(\frac{Y_x}{C_x}\right) \cdot \left(\frac{dM_z}{dt}\right) / Q \quad (10)$$

Where

Q is the rate of airflow into which the gas is expelled (m^3/s).

For most toxic gases, a quantity called the IDLH value represents the concentration of that gas that is immediately dangerous to life and health. The Occupational Safety and Health Administration (OSHA) defines an IDLH value in its hazardous waste operations and emergency response regulation [29 CFR 1910.120] as an atmospheric concentration of any toxic, corrosive, or asphyxiate substance that poses an immediate threat to life or would cause irreversible or delayed adverse health effects or would interfere with an individual's ability to escape from a dangerous atmosphere [16]. The IDLH value for a toxic gas represents a benchmark that signals the transition to an imminent hazard condition. Dividing Eq. (10) by the IDLH value (in ppm) for toxic species X, an estimate of the toxic severity of the air into which the gas is expelled can be obtained. The parameter that results is called the relative toxic hazard due to gas species X, denoted by $(RTH)_X$, and is given by

$$(RTH)_x = \left(\frac{Y_x}{(IDLH)_x C_x}\right) \cdot \left(\frac{dM}{dt}\right)/Q \quad (11)$$

For most combustible materials, more than one toxic gas is produced. If it is assumed that the cumulative toxic effects from all the toxic gases are additive, then the total toxic hazard due to the combustion of sample material Z is called the total relative toxic hazard, denoted by $(TRTH)_Z$, and is given as the summation of all $(RTH)_X$ values

$$(TRTH)_z = \sum (RTH)_x \quad (12)$$

It becomes convenient, then, to define a toxicity parameter for combustible material Z as

$$(TOX)_z = \sum Y_x/((IDLH)_x C_x) \quad (13)$$

and, combining Eqs. (11)–(13), the total relative toxic hazard for material Z can be expressed as

$$(TRTH)_z = (TOX)_z \cdot (dM_z/dt)Q \quad (14)$$

The total rate of mass loss for material Z is equal to the product of total surface area burning, S_Z, (m^2) and the mass loss rate per unit surface area, $(M_Z)''$, ($g/(m^2\ s)$). The maximum surface area that is burning can be estimated as follows:

$$S_z = (n_z \rho_z W h (V_f)_z)/(M_z)'' \quad (15)$$

Where

η_Z is the fraction of sample mass that is actually consumed as combustion fuel;

ρ_Z is the bulk density of the sample material (g/m^3);

W is the width of the sample surface (m);

h is the thickness of the sample (m); and

$(V_F)_Z$ is the rate of flame spread along the length of the sample material (m/s).

Since $(dM_Z/dt) = S_Z \ldots (M_Z)''$, the following expression results for the total relative toxic hazard

$$(TRTH)_z = (TOX)_z \cdot (n_z \rho_z W h (V_f)_z)/Q \quad (16)$$

Eq. (16) provides an estimate of the level of toxicity that could be achieved during an actual fire. This toxicity estimation is important as it relates to both the chemical composition and the flame-resistant properties of a material.

For the experiments described in this report, a simpler ratio, similar to that defined in Eq. (11) above, and denoted as the toxicity index (TI), is defined as the sum of the average maximum gas concentrations, X (ppm), divided by the IDLH value for the individual gases, or

$$T1 = \sum X(ppm)/(IDLH)_x \quad (17)$$

Since the total mass loss, Δm, of the sample was also measured during the experiments, it is also possible to form the ratio, TI/Δm, which is similar to the expression for $(TOX)_Z$ defined in Eq. (13) above.

4. Combustion-generated aerosols and the smoke hazard parameter

As noted in previous studies, aerosols generated from fires have been found to be fractal, or fractal-like, aggregates that are composed of significant numbers of smaller primary particles with morphologies that depend upon the stage of the combustion [14,15]. For flaming combustion, these aggregates appear as elongated chains with primary particles showing very little overlap, and are typically defined by a fractal dimension, D_f, of approximately 1.8 to 1.9. For smoldering combustion, the aggregates appear more clumped with significant overlap and fractal dimensions in the vicinity of 2.1 to 2.2. The degrees of overlap for the different particles are especially important since the overlap determines to a large extent the effective surface area available for adsorption of reactive and potentially toxic gases that could eventually be transferred to tissue within the respiratory tract when persons are exposed to these aerosols.

Before looking at structure properties of these aerosols that may have some relationship to toxicity, it should be noted that smoke obscuration represents a major hazard during fire

emergencies that drastically reduces a person's ability to safely evacuate an affected fire area. In these experiments, data on the mass scattering and mass extinction coefficients were acquired that allow for the determination of transmission of light (and hence, obscuration) as a function of the mass concentration of the aerosol. For aerosols from smoldering fires, the majority of total light extinction comes from light that is scattered by aerosols with low carbon content, while for aerosols from flaming fires, the major portion of total light extinction comes from light that is absorbed by aerosols with high carbon content. For smoldering fires, the average values of mass scattering coefficient, σ_{sca}, mass extinction coefficient, σ_{ext}, and by difference, the mass absorption coefficient, σ_{abs}, are shown in Table 3 below in units of m^2/g.

For aerosols from flaming fires, the data are shown in Table 4.

Also shown in Tables 3 and 4 is the light extinction, σ_{vis}, measured using a photodiode with a response that mimics the response of the human eye; the albedo, the ratio of scattering to extinction; and the mass of black carbon (BC) in the aerosol and the ratio of BC mass to total aerosol mass concentration. For aerosols from smoldering fires, the average mass extinction coefficient is approximately 12.9 m^2/g, of which roughly 80%, or 10.2 m^2/g, is due to scattering. For the visible extinction, a value of 5.7 m^2/g was measured, but it is felt that this low value may be due to some scattering of light that the visible photodiode receives because of its wide field of view. It is also worth noting that the average BC concentration for these aerosols is only 0.092 mg/m^3, or less than 0.6% of the total aerosol mass.

For aerosols from flaming fires, the average mass extinction coefficient is 20.4 m^2/g and of this, 15.7 m^2/g, or about 77%, is due to absorption rather than scattering. The visible mass extinction coefficient is also much higher by a factor of almost 3, at 15.7 m^2/g. The higher absorption also correlates well with the higher average BC mass concentration of 8.7 mg/m^3, or about 43% of the total aerosol mass concentration. The extinction coefficients are related to a parameter called the optical density, OD, in units of m^{-1}, by the expression

$$OD=(\sigma_{ext} \cdot M)/2.303 \quad (18)$$

where M is the aerosol mass concentration in g/m^3. From previous research the critical optical density for human escape is 0.217 m^{-1}, and from the above average values, this level is reached for smoldering fires at a mass concentration of about 38 mg/m^3, and at about 24 mg/m^3 for smoke from flaming fires [Oh, 1989; Jin, 1979]

While aerosol mass concentrations have typically been the metric used by hygienists to assess adverse health effects, it is highly probable that a better metric, at least for ultrafine aerosols with diameters less than about 350 nm, is the total surface area or, perhaps, the total surface area per aggregate. Because combustion aerosols have different morphologies and, hence, varying degrees of overlap, the exposed surface areas per fractal aggregate become a function not only of the size and number of primary particles but also the shape of the aggregate and the degree of overlap of the primary particles. To account for these effects,

previous research was used to estimate the overlap as a function of the fractal dimension, D_f [15]. In the experiments conducted here, the number concentrations of the aerosol, the fractal dimensions, primary particle diameters, and numbers of primary particles per aggregate are measured. Using the approximations for overlap the actual, or effective, aggregate surface areas and total surface areas may be calculated [15]. The average data for these parameters for the flaming experiments are shown in Table 5 below.

Correlations were found between both the effective aggregate surface area per mass of sample consumed and the toxicity index per mass of sample consumed, and the total surface concentration per mass of sample consumed and the toxicity index per mass of sample consumed. These correlations are shown in Figs. 4 and 5 for the effective aggregate surface area and the total aerosol surface area, respectively.

Although there is scatter in both correlations shown in Figs. 4 and 5, there do appear to be relationships between the aerosol surface areas and the toxic gas concentrations that are in need of further investigation. But irrespective of these correlations, it should be expected that the larger the aggregate and total surface areas, the greater the hazard, since it is the aerosol surfaces that are in contact with the tissues that line the respiratory tract.

The smoke parameters of significant interest from these experiments are the mass extinction coefficient, σ_{ext}, which is directly related to the level of smoke obscuration that these burning materials produce, and the total aerosol surface area per unit mass of combustible consumed, which correlates linearly with the toxicity indices (Fig. 3). These two parameters can be combined to generate a smoke hazard parameter, SHP, given by the equation

$$SHP = 1 \times 10^{-6}\{\sigma_{ext} \cdot (S_{TOT})_{eff}/ \cdot m\}^{1/2} \quad (19)$$

From these experiments conducted in the smoke chamber, a toxicity index (TI) and a smoke hazard parameter (SHP) were derived that, combined, represent the hazards of smoke obscuration and toxicity of the combustion products generated from the various materials tested. More details of this part of the research can be found in the paper by Litton and Perera [2015] [15]. Only the final values will be reported and used here as part of the development of an overall fire hazard summary. The toxicity index, TI, represents a weighted sum of the concentrations of toxic gases measured during these experiments, and the final values that were obtained are listed in Table 6. Also shown in Table 6 are the TI values per unit mass of sample weight loss measured during the experiments, TI/ΔM.

In addition, using the data in Table 6, it is possible to rate these materials as to the potential toxic hazard they present. This rating is shown in Table 7, where the rating is based upon either TI or TI/ΔM for the flaming experiments only, since it was for this stage of combustion that the highest gas levels were reached. With only one major exception, sample #6, and to a slightly less extent, sample #7, these rankings are in reasonable agreement with each other.

Similarly, for the combustion-generated aerosols, the SHP, defined in Eq. (19) above can subsequently be used to rank the materials relative to the resultant smoke hazard. The result is shown in Table 8.

5. Discussion and summary

Overall, data presented in this report can be used to derive parameters related to overall fire hazard, which can be used to assist in assessing the relative fire safety of combustible mine materials.

From the radiant panel experiments, two essentially equivalent parameters were derived, *TP1* and *TP4*, which may be used to assess the risk of ignition of combustible mine materials and their subsequent fire intensities. From the smoke chamber experiments, the toxicity index, *TI*, or the toxicity index per unit mass of material consumed during combustion, $TI/\Delta m$, and the smoke hazard parameter, SHP, were derived, which can be used to partially assess the hazardous atmosphere created when these materials burn. Given these various parameters, the total fire hazard parameter, *HAZ*, can then be expressed as some functional combination of these, or

$$HAZ = HAZ(TP1, TI, SHP)$$

It is perhaps best to utilize these parameters to define, within each parameter category, three levels of hazard: low, medium, and high. To see how this might work, it is instructive to reproduce the three ranking tables along with their respective values. This is shown in Table 9.

For the thermal hazard parameter, inspection of the relative values of TP1 and TP4 in Table 9 indicates that TP1 may be the better parameter to use, with values of TP1 less than 55 a low hazard, values from 56 to 100 a medium hazard, and values greater than 100 a high hazard. For the toxicity parameter, TI/ΔM, values less than 0.65 would be classified as low hazard, values from 0.65 to 1.0 as medium hazard, and values greater than 1.0 as high hazard. For the smoke hazard parameter, inspection of Table 8 would indicate that values less than 2 would be low hazard, values between 2 and 3 medium hazard, and values 3 or greater high hazard. Using this approach, Table 10 can be constructed, summarizing which materials fall into the different hazard levels for each of the three parameter categories.

Using these comparisons, it is obvious that some materials are consistently in the low hazard level, such as samples 3 and 11, which appear in two parameter categories as low hazard and in one category as a medium hazard. Similarly, some samples appear consistently in the high hazard level, such as 2, 5, 6, 8, 14, 15, and 16. At the minimum, this approach would eliminate many combustible materials that pose relatively high hazards for at least two of the parameters.

Regardless of exactly how such parameters may ultimately be used, it is proposed that they represent realistic estimates and provide a framework for comparison of the individual

hazards that different materials may present. These results clearly indicate that the testing and evaluation of other combustible materials is warranted.

References

1. Apte, VB. Flammability testing of materials used in construction, transport and mining. CRC Press: Woodhead Publishing; 2006. p. 459
2. Tewarson A. Flammability parameters of materials: ignition, combustion, and fire propagation. J Fire Sci. 1994; 12:329–56.
3. Tewarson A. Ventilation effects on combustion products. Toxicology. 1996; 115(1–3):145–56. [PubMed: 9016749]
4. Tewarson, A., Abuisa, IA., Cummings, DR., Ladue, DE. Characterization of the ignition behaviour of polymers commonly used in the automotive industry. Fire Safety Science – Proceedings of the Sixth International Symposium; 2000; p. 991-1002.
5. Tewarson, A. Smoke emissions in fires. Proceedings of the Ninth International Symposium; 2008; p. 1153-64.
6. Litton CD, Perera IE, Teacoach KA. The analysis and quantification of toxic gases and smoke released from the combustion of common mine materials. Fire Safety J. 2015 Dec 18.
7. Paciorek KL, et al. Determination of the products of the oxidative thermal degradation of variously treated woods and mine materials. US Bureau of Mines Open File Report. 1980; 4–82:169.
8. Paciorek KL, Kratzer RH, Nakahara JH, Ahmed SR. Products of the oxidative thermal degradation of mine stoppings and mine reinforcing materials. US Bureau of Mines Open File Report. 1983; 24–87:124.
9. Harteis, SP., Litton, CD., Thomas, RA. Determination of the Fire Hazards of Mine Materials Using a Radiant Panel, Preprint 15–128. SME Annual Meeting; Denver, CO. 2015;
10. Edwards JC, Morrow GS. Development of coal combustion sensitivity tests for smoke detectors. United States Department of Interior Report of Investigation. 1995; 9551:1–12.
11. DeRosa MI, Litton CD. Determining the relative toxicity and smoke obscuration of combustion products of mine combustibles. US Bureau of Mines Report of Investigations. 1989; 9274:11.
12. Oh C, Sorensen CM. The effect of overlap between monomers on the determination of fractal cluster morphology. J Colloid Interface Sci. 1997; 193:17–25. [PubMed: 9299084]
13. Jin T. Visibility through fire smoke. J Fire Flam. 1978; 9:135–57.
14. Litton, CD., Mura, KE., Thomas, RA., Verakis, HC. Flammability Studies of Noise Abatement Materials Used in Cabs of Large Mobile Mining Equipment. Proceedings Fire and Materials Conference; San Francisco, CA. 2003;
15. Perera IE, Litton CD. Quantification of optical and physical properties of combustion-generated carbonaceous aerosols (smaller than PM2. 5) using analytical and microscopic techniques. Fire Technol. 2015; 51(2):247–69. [PubMed: 27546898]
16. OSHA. CFR. 1910.

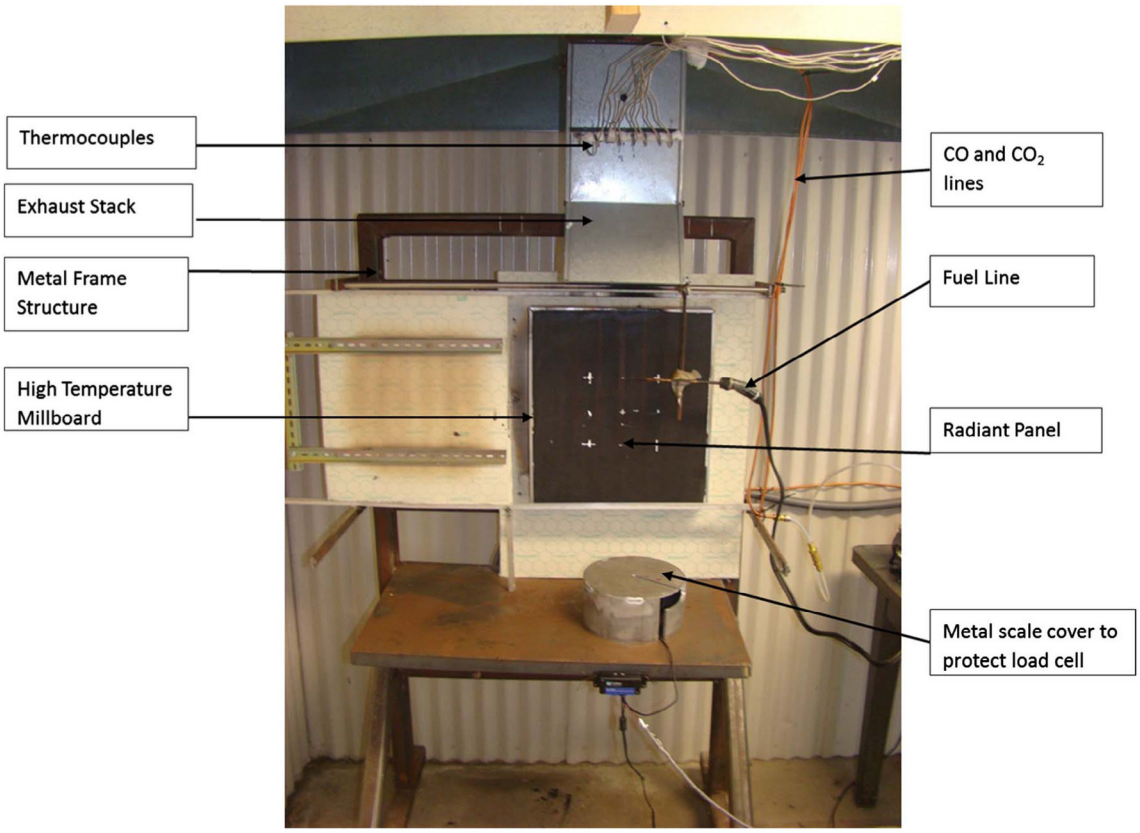

Fig. 1.
Radiant panel apparatus.

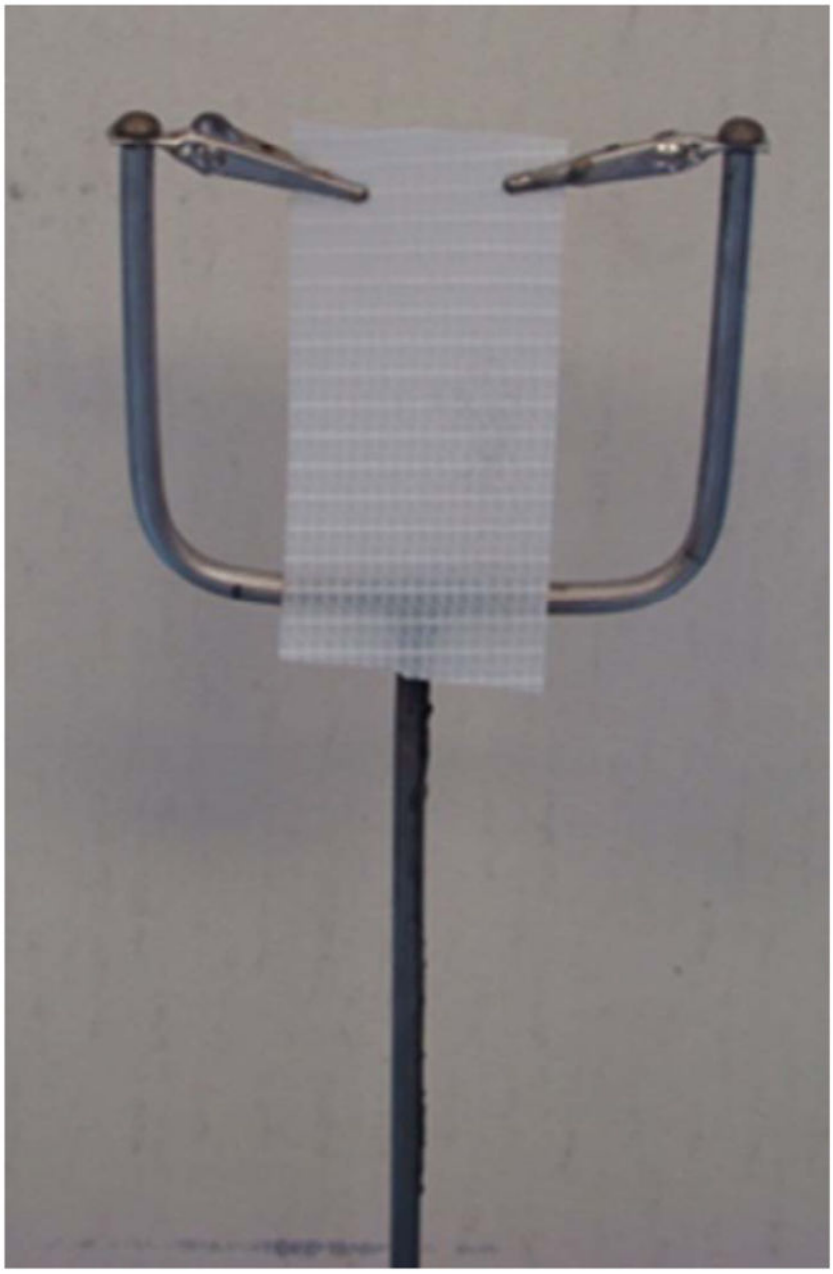

Fig. 2.
Metal holder with clips holding brattice material.

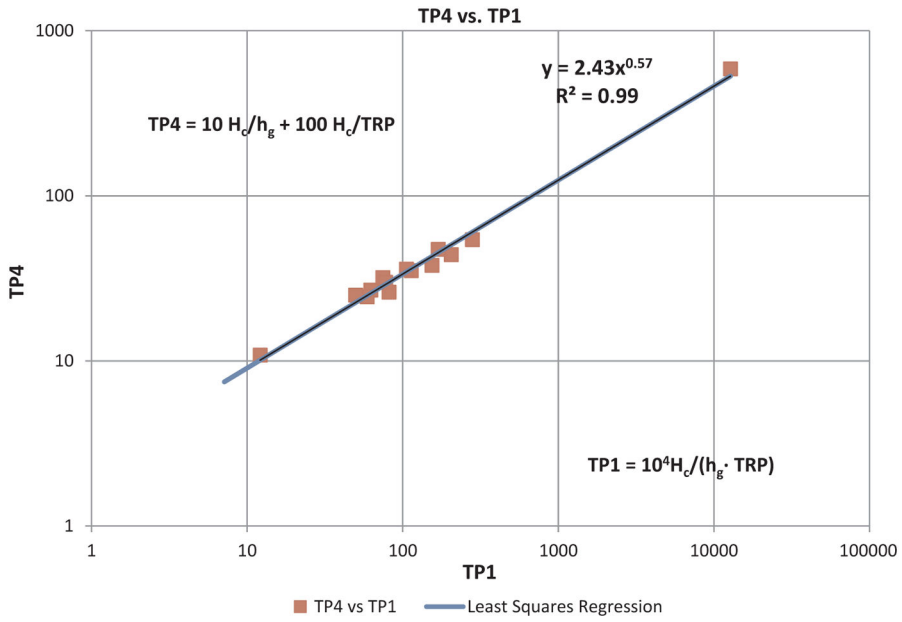

Fig. 3.

The average values of the additive thermal parameter, *TP4*, plotted vs the average value of the multiplicative thermal parameter, *TP1*.

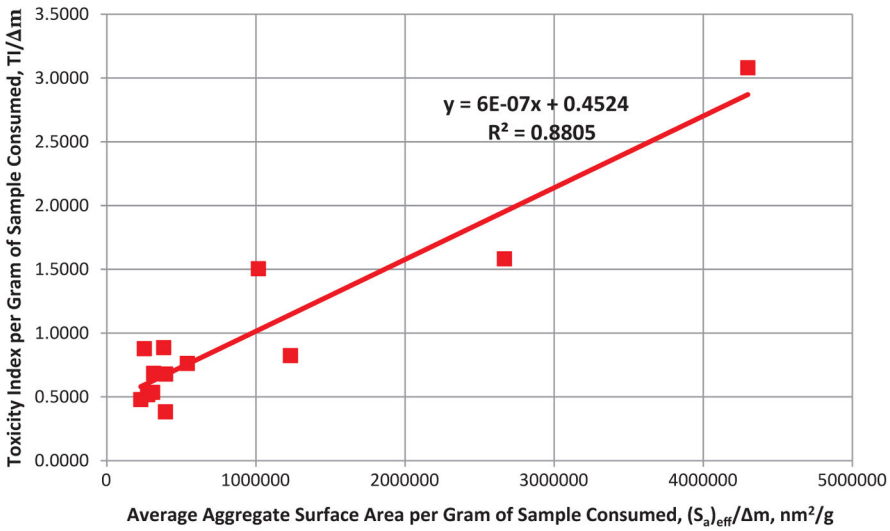

Fig. 4.

Correlation between the aggregate surface area and toxicity index.

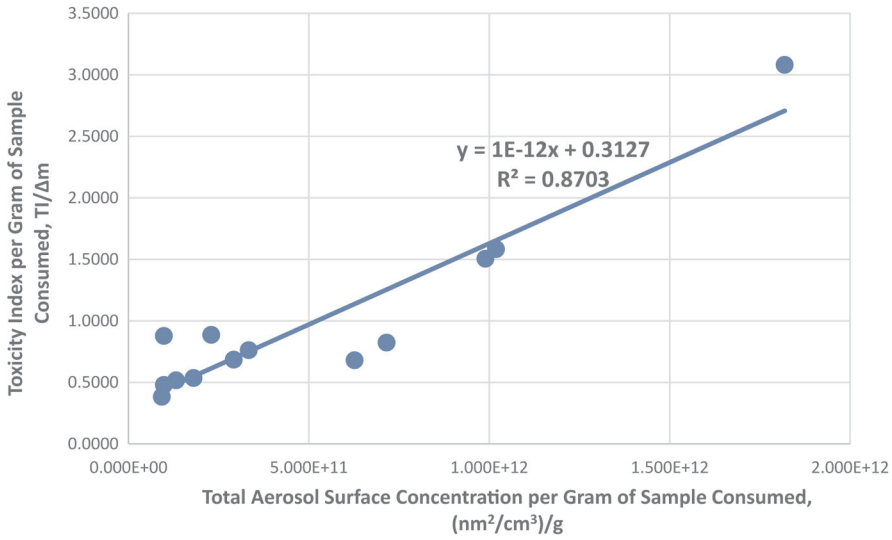

Fig. 5.
Correlation between the total aerosol surface concentration and the toxicity index.

Table 1

Average values of thermal parameters, TP1 and TP4, calculated for each material.

Combustible Material	Sample Number/Number Designation	TP1	TP4
Brattice 1	1	82	26
Brattice 2	2	281	54
Brattice 3	3	N/A	15
Brattice 4	4	12	11
Semi-rigid Sealant	5	114	35
Foam sealant	6	12,783	587
PVC conveyor belt 1	7	75	32
PVC conveyor belt 2	8	154	38
SBR conveyor belt 1	9	N/A	17
SBR conveyor belt 2	10	62	27
SBR conveyor belt 3	11	78	30
SBR conveyor belt 4	12	59	24
SBR conveyor belt 5	13	50	25
pine	14	205	44
select pine	15	169	47
oak	16	106	36

Table 2

Ranking of the materials tested from low hazard to high hazard based upon the average values obtained for TP4 and TP1, respectively.

Combustible Material	Number Designation	Sorted on TP4	Sorted on TP1
Brattice 1	1	4	4
Brattice 2	2	3	N/A
Brattice 3	3	9	N/A
Brattice 4	4	12	13
Semi-rigid Sealant	5	13	12
Foam sealant	6	1	10
PVC conveyor belt 1	7	11	7
PVC conveyor belt 2	8	7	11
SBR conveyor belt 1	9	10	1
SBR conveyor belt 2	10	5	16
SBR conveyor belt 3	11	16	5
SBR conveyor belt 4	12	8	8
SBR conveyor belt 5	13	14	15
pine	14	15	14
select pine	15	2	2
oak	16	6	6

Table 3

Optical scattering, absorption, and extinction data for smoldering fire experiments.

							Average over BC Peak	
Combustible Material	**Sample Number**	**σ_{ext}**	**σ_{sca}**	**σ_{abs}**	**σ_{vis}**	**Albedo**	**M_{BC}(mg/m^3)**	**M_{BC}/M_{TOT}**
Vintex Brattice	1	11.7	11	0.689	5.62	0.941	0.123	0.006
BC 77/03 Brattice	2	11.2	9.39	1.80	5.14	0.839	0.092	0.005
Airstop 100 Clear Brattice	3	14.1	9.8	4.29	5.78	0.695	0.031	0.002
07-BA04001 Brattice	4	12.3	6.4	5.89	5.49	0.521	0.069	0.009
Line-X hard Sealant	5	17.1	10.6	6.53	6.11	0.618	0.147	0.005
Silent Seal Foam	6	12.4	11.5	0.80	6.43	0.935	0.057	0.003
8020–0168 M (A)	7	13.5	11.1	2.43	6.11	0.820	0.073	0.007
0000-0007 PVC (B)	8	14.7	11.7	2.98	6.19	0.797	0.055	0.003
Phoenix (C)	9	10.2	8.92	1.32	4.94	0.871	0.138	0.010
Harry's Belt (D)	10	14.4	10.9	3.50	5.68	0.757	0.039	0.003
Belt 6115-017,704 (E)	11	10.3	9.53	0.76	5.34	0.927	0.068	0.004
Belt 6115-0184 (F)	12	14	11.8	2.14	5.87	0.847	0.171	0.009
Belt 6115-3003 M (G)	13	12.2	10.4	1.9	5.43	0.845	0.139	0.009
	Average	12.9	10.2	2.70	5.70	0.801	0.092	0.006

Table 4

Optical scattering, absorption, and extinction data for flaming fire experiments.

							Average over BC Peak	
Combustible Material	**Sample Number**	**σ_{ext}**	**σ_{sca}**	**σ_{abs}**	**σ_{vis}**	**Albedo**	**M_{BC}(mg/m^3)**	**M_{BC}/M_{TOT}**
Vintex Brattice	1	22.14	6.92	14.3	10.4	0.312	6.37	0.380
BC 77/03 Brattice	2	15.1	1.60	13.7	8.47	0.105	13.1	0.407
Airstop 100 Clear Brattice	3	25.5	4.28	21.3	14.8	0.168	17.7	0.355
07-BA04001 Brattice	4	15	8.07	6.24	7.86	0.538	5.34	0.387
Line-X hard Sealant	5	7.87	0.97	6.90	5.43	0.123	11.6	0.341
Silent Seal Foam	6	20.6	5.79	14.8	12.9	0.281	6.55	0.561
8020-0168 M (A)	7	19.4	3.36	16.0	17.1	0.174	5.35	0.306
0000-0007 PVC (B)	8	23.7	1.49	22.2	18.2	0.063	10.9	0.657
Phoenix (C)	9	26.1	5.80	20.3	17.1	0.222	8.28	0.396
Harry's Belt (D)	10	24.3	4.90	19.4	16.1	0.202	7.49	0.510
Belt 6115-017,704 (E)	11	26.5	4.63	21.9	14.3	0.175	5.97	0.495
Belt 6115-0184 (F)	12	19.8	5.92	13.8	19.5	0.300	8.59	0.506
Belt 6115-3003 M (G)	13	19.3	5.57	13.8	13.1	0.288	5.78	0.290
	Average	20.4	4.56	15.7	13.5	0.227	8.69	0.430

Table 5

Average aggregate properties that led to correlations with gas toxicity.

Sample Number	d_p (nm)	n_p	N	D_f	Effective Surface Fraction	Mass Loss Δm (g)	$(S_a)_{eff}$/Δm nm^2/g	$(S_{tot})_{eff}$/Δm (nm^2/cm^3)/g	Flaming TI/Δm
1	48.1	361	618,406	2.00	0.370	1.80	549,390	3.335E + 11	0.762
2	146	75	581,333	1.95	0.492	2.02	980,421	9.846E + 10	0.823
3	107	65	235,871	1.91	0.466	2.80	407,756	1.806E + 11	0.383
4	50.0	911	382,050	1.81	0.643	1.73	1,801,751	2.297E + 11	1.58
5	89.6	167	973,900	1.86	0.509	2.11	1,149,753	1.321E + 11	1.50
6	84.2	109	423,151	1.81	0.630	0.35	3,852,067	2.920E + 11	3.08
7	53.7	226	432,113	1.83	0.619	5.57	233,465	7.157E + 11	0.479
8	26.7	629	1,591,849	1.69	0.844	3.02	371,953	6.269E + 11	0.679
9	47.4	429	589,043	1.99	0.377	3.72	240,448	9.265E + 10	0.536
10	36.7	429	392,776	1.84	0.560	4.06	256,110	1.019E + 12	0.878
11	37.3	429	483,279	1.86	0.509	3.49	257,918	9.897E + 11	0.517
12	42.8	344	602,946	1.85	0.532	2.76	361,071	9.835E + 10	0.886
13	32.5	502	931,799	1.83	0.586	3.11	303,952	1.819E + 12	0.684

Table 6

Average values of TI and TI/ΔM for 13 sample materials tested.

		Smolder		Flaming	
Sample Number	**Combustible Material**	**Average TI**	**Average TI/ΔM**	**Average TI**	**Average TI/ΔM**
1	Vintex Brattice	0.187	0.199	1.16	0.762
2	BC 77/03 Brattice	0.207	0.309	1.81	0.823
3	Airstop 100 Clear Brattice	0.417	0.423	1.01	0.383
4	07-BA04001 Brattice	0.146	0.327	2.70	1.583
5	Line-X hard Sealant	0.327	0.342	2.76	1.504
6	Silent Seal Foam	0.155	0.259	1.09	3.080
7	8020-0168 M (A)	0.235	0.472	2.08	0.479
8	0000-0007 PVC (B)	0.183	0.215	2.05	0.679
9	Phoenix (C)	0.389	0.481	2.30	0.536
10	Harry's Belt (D)	0.283	0.743	3.02	0.878
11	6115-017,704 (E)	0.281	0.578	1.80	0.517
12	6115-0184 (F)	0.353	0.900	2.45	0.886
13	6115-3003 M (G)	0.297	0.578	1.99	0.684

Table 7

Toxicity hazard ranking based upon either the flaming TI or the flaming TI/ΔM from low to high and their respective values.

Sample #	Average Flame TI	Sample #	Average Flame TI/ΔM
3	1.01	3	0.329
6	1.09	7	0.479
1	1.16	11	0.517
11	1.81	9	0.536
2	1.81	8	0.679
13	1.99	13	0.684
8	2.05	1	0.762
7	2.08	2	0.823
9	2.30	10	0.878
12	2.45	12	0.886
4	2.70	5	1.504
5	2.76	4	1.583
10	3.02	6	3.080

Table 8

Ranking of the sample materials according to their smoke hazard parameter, SHP.

Sample number	SHP
7	1.38
3	1.54
10	1.55
11	1.87
12	2.13
9	2.17
13	2.38
1	2.72
5	2.79
2	3.31
8	3.86
4	3.91
6	6.12

Table 9

Hazard rankings using the three parameters discussed previously as Tables 2, 7 and 8.

Sample Number	Average TP1	Average TP4				
4	12.1	10.8				
3	N/A	15.2	Sample number	Average		
9	N/A	17.0		TI/ΔM	Sample number	SHP
12	59.0	24.4	3	0.329	7	1.38
13	49.9	25.0	7	0.479	3	1.54
1	81.7	26.1	11	0.517	10	1.55
10	62.4	26.9	9	0.536	11	1.87
11	77.8	29.9	8	0.679	12	2.13
7	74.5	31.9	13	0.684	9	2.17
5	113	35.2	1	0.762	13	2.38
16	104	36.0	2	0.823	1	2.72
8	154	37.9	10	0.878	5	2.79
14	205	44.0	12	0.886	2	3.31
15	169	47.4	5	1.50	8	3.86
2	281	54.2	4	1.58	4	3.91
6	12,783	587	6	3.08	6	6.12

Table 10

Results of ranking the various combustible materials into three distinct hazard levels.

HAZARD PARAMETER	HAZARD LEVEL		
	LOW	MEDIUM	HIGH
TP1	4, 3, 9, 13	12, 1, 10, 11, 7	5, 16, 8, 14, 15, 2, 6
TI	3, 7, 11, 9	8, 13, 1, 2, 10, 12	5, 4, 6
SHP	7, 3, 10, 11	12, 9, 13, 1, 5	2, 8, 4, 6